Supporting Information

Accelerating Electrochemically Catalyzed Nitrogen Reductions on Metalloporphyrin-Mediated Metal-Nitrogen-Doped Carbon (M-N-C) Catalysts

Xinyi Dong, Weihua Zhu*, Xu Liang*

School of Chemistry and Chemical Engineering, Jiangsu University, Zhenjiang 212013, P. R. China

Corresponding to: E-mail: liangxu@ujs.edu.cn (to X. Liang); E-mail: sayman@ujs.edu.cn (to W. Zhu)

1.1 Chemicals and materials

Analytical grade pure reagents anhydrous sodium sulfate, ammonium chloride, sodium salicylate, trisodium citrate, isopropanol, acetone, anhydrous ethanol, *p*-dimethylaminobenzaldehyde, sodium hydroxide, Nafion solution and reduced graphene oxide were purchased from Shanghai Aladdin Biochemical Technology Co., Ltd. Hydrochloric acid and sulfuric acid were obtained from Sinopharm Chemical Reagent Co. Ltd. Sodium nitroprusside dihydrate was purchased from ShangHai D&B Biological Science and Technology Co. Ltd. Tetraphenyl iron porphyrin was purchased from Alfa Aesar (China) Chemical Co., Ltd. Nickel-, manganese-, zinc-, cobalt- and copper-porphyrins were synthesized by experiments. All commercial chemicals used in this experiment were not further purified. Deionized water was used in all experiments.

1.2 Preparation of Catalysts

1.2.1 Preparation of MTPP@rGO-t (M=Fe, Ni)

First, 30 mg of MTPP (M=Fe，Ni) were dissolved in 15mL dichloromethane solution via sonicating for 15 min to form a clear solution. 20 mg of rGO was then added and sonicated together for 30 min to obtain a suspension. The mixture was stirred continuously at room temperature for 12 hours. After dried on a rotary evaporator, the obtained powder, which is denoted as MTPP@rGO (M = Fe, Ni), was placed in a porcelain boat and annealed in the tube furnace with pure Ar flow. Pyrolysis temperature procedure was set as follows： firstly, raise the temperature to 500°C at the rate of 5 °C min^{-1}; then continue to raise the temperature to t °C (t = 600/700/800/900) at the rate of 10°C min^{-1}; afterwards, maintain the temperature for 2 hours, then lower the temperature to 500 °C at the rate of 10 °C min^{-1}, continue to lower the temperature to 300 °C at the rate of 5 °C min^{-1}, and then wait for it to cool naturally to room temperature. And finally, the pyrolysis products were stirred in 0.5 M H_2SO_4 for 12h to remove the impurities, and then washed for several times with isopropanol to remove sulfuric acid, and dried on a rotary evaporator to eventually obtained MTPP@rGO-t (M = Fe, Ni; t=600/700/800/900).

1.2.2 Preparation of $Fe_{0.95}M_{0.05}$TPP@rGO-800 (M=Mn, Ni, Zn, Cu, Co)

$Fe_{0.95}M_{0.05}$TPP@rGO (M=Mn, Ni, Zn, Cu, Co) was prepared in parallel by the same method as that for MTPP@rGO (M = Fe， Ni), except for using 28.5 mg of FeTPP and 1.5 mg of MTPP (M = Mn, Ni, Zn, Cu, Co) to achieve the targeted dual-metal-atom catalysts. The obtained $Fe_{0.95}M_{0.05}$TPP@rGO (M = Mn, Ni, Zn, Cu, Co) was then annealed at 800 °C by the pyrolysis temperature procedure identical to that for MTPP@rGO-t , after which the pyrolysis products were treated with acid and isopropanol as that in 1.2.1 to eventually obtained $Fe_{0.95}M_{0.05}$TPP@rGO-800 (M =Mn, Ni, Zn, Cu, Co).

1.2.3 Preparation of $Fe_{1-x}Ni_x$TPP@rGO-800（x = 1%, 3%, 5%, 7%）

Control the mass ratio of NiTPP to FeTPP at 1%, 3%, 5% and 7% to prepare $Fe_{1-x}Ni_x$TPP@rGO-800 (x=1%, 3%, 5%, 7%) according to the same method as that for FeTPP@rGO-800.

1.3 Characterization

Powder X-ray diffraction (XRD) analysis was performed by a Shimadzu 6100 X-ray diffractometer equipped with high intensity Cu-Kα radiation. Scanning electron microscope (SEM) was collected by a JSM-6010PLUS/LA thermal field emission scanning electron microscopy (JEOL, Japan). Fourier transform infrared (FT-IR) spectra were recorded by Nicolet Nexus 470 FT-IR instrument (KBr tableting). X-ray photoelectron spectroscopy (XPS) was carried out on a Thermo Escalab 250Xi XPS system with Al Kα radiation. Raman measurements were made on a Thermo Scientific DXR Smart Raman spectrometer using a 532 nm laser.

1.4 Preparation of carbon paper electrode

The 0.5×0.5 cm^2 carbon paper was sonicated respectively in 10 mL of absolute ethanol, acetone and absolute ethanol again for 10 min, and dried at room temperature. 2 mg catalyst and 40 µL of Nafion solution were dispersed in 760 µL of isopropyl alcohol by sonicating for 30 min to form a homogeneous catalyst ink. Afterwards,100 µL of the ink was pipetted on each side of the carbon paper respectively, and dried under room temperature. The carbon paper electrode with catalyst loading of 1.0 mg cm^{-2} was obtained.

1.5 Electrochemical measurements

The Nafion 117 membrane was immersed in 5 wt% H_2O_2 and 5 wt% H_2SO_4 solution at 80 ℃ for 1h respectively, and the treated Nafion 117 membrane was then used to separate the airtight H-cell connected to an electrochemical workstation (CHI 730D). The conventional three-electrode system was adopted for electrochemical measurement by using carbon paper with catalyst as a working electrode and graphite rod as a counter electrode, and saturated Ag/AgCl (saturated KCl) electrode as a reference electrode. 25 mL of 0.1M Na_2SO_4 were added respectively to the cathodic and anodic cell. The electrolyte was purged with high-purity N_2 or Ar before each measurement. In order to eliminate possible NH_3 and NO_x pollutants in the feeding gas, N_2 or Ar shall pass through the concentrated sulfuric acid gas washing device and alkali lime drying device before purged to the cathodic cell. NH_3 produced by the reaction mainly exists in the neutral electrolyte solution in the form of NH_4^+. Potentials observed using Ag/AgCl were converted to reversible hydrogen electrode (RHE) using the Nernst equation $E_{RHE} = E_{Ag/AgCl} + 0.059pH + E^0_{Ag/AgCl}$, where $E_{Ag/AgCl}$ is the experimetally determined potential using Ag/AgCl reference electrode; $E^0_{Ag/AgCl}$ is 0.199V at 25℃. All experiments were carried out at room temperature.

1.6 Determination of NH_3.

In this work, indophenol blue spectrophotometry method was used to detect and quantify NH_3 produced by electrochemical NRR. Prepare the following solutions: 1) Oxidizing solution: 0.05 M NaClO solution (6-14% available chlorine); 2) Coloring solution: 1 M NaOH solution containing 5 % sodium salicylate and 5 % trisodium citrate dehydrate; 3) Catalyst solution: 1.01 g

$Na_2[Fe(CN)_5NO]$ $2H_2O$ diluted to 100 mL with deionized water; 4) Standard solution: ammonium chloride (NH_4Cl) in a serious of concentrations. In detail, 2 mL of oxidizing solution, 1 mL of coloring solution, and 0.2 mL of catalyst solution were added into the 2 mL electrolyte, which was taken from the cathodic cell after NRR. The obtained mixture solution was diluted to 10 mL using the deionized water. After standing in dark at room temperature for 2 h, the solution was measured on a UV-vis spectrophotometer. The maximum UV-vis absorption was measured at 689 nm. The concentration-absorbance curves were calibrated using standard NH_4Cl solution in a series of concentrations at maximum absorbance via the same procedure as mentioned above. The fitting curve (*Figure S1*, see ESI) is $y = 0.08051\ x + 0.01435$, which shows a good linear relation between absorbance with NH_3 concentration ($R^2 = 0.9999$) and can be used to detect the quantity of NH_3 in subsequent tests.

1.7 Determination of hydrazine (N_2H_4)

Hydrazine is also a possible product in addition to NH_3 in the process of electrochemical NRR, and it was detected by UV-vis spectroscopy using the method of Watt and Chrisp. The color reagent was prepared by a mixed solution of 4 g of *p*-dimethylaminobenzaldehyde, 20 mL of concentrated hydrochloric acid and 200 mL of absolute ethanol. Specifically, 5 mL of color reagent was added into 5 mL of electrolyte, which was taken from the cathodic cell after NRR. After standing in dark at room temperature for 20 min, the solution was measured on a UV-vis spectrophotometer. The maximum UV-vis absorption was measured at 460 nm. The concentration-absorbance curves were calibrated using standard N_2H_4 H_2O solution in a series of concentrations. As shown in *Figure S2*, the fitting curve shows a good linear relation between absorbance with N_2H_4 concentration ($R^2 = 0.9999$), which can be used to detect the quantity of N_2H_4 in subsequent tests.

1.8 Computational formulas of NH_3 yield rate and Faradaic efficiency

NH_3 yield and Faradaic efficiency are important indicators to measure the performance of catalysts. The NH_3 yield rate is calculated as follows:

$$NH_3\ yield\ rate = \frac{C_{NH_3} \times V}{t \times m}$$

Where C_{NH3} (μg/mL) is the concentration of the produced NH_3, V(mL) is the volume of electrolyte, *t*(h) is the reduction reaction time, *m* (mg) is the mass of the catalyst. The Faradaic efficiency of NRR is defined as the percentage of the electric charge consumed by the synthesis for NH_3 to the total electric charge in the electrolysis process. Assuming that three electrons are consumed to produce an NH_3 molecule, the Faradaic efficiency can be calculated as follows:

$$FE = \frac{3 \times F \times C_{NH_3} \times V}{17 \times Q} \times 100\%$$

Where *F* is the Faradaic constant (96485 C/mol)，*Q* (C) is the quantity of charge integrated by the chronoamperometry curve.

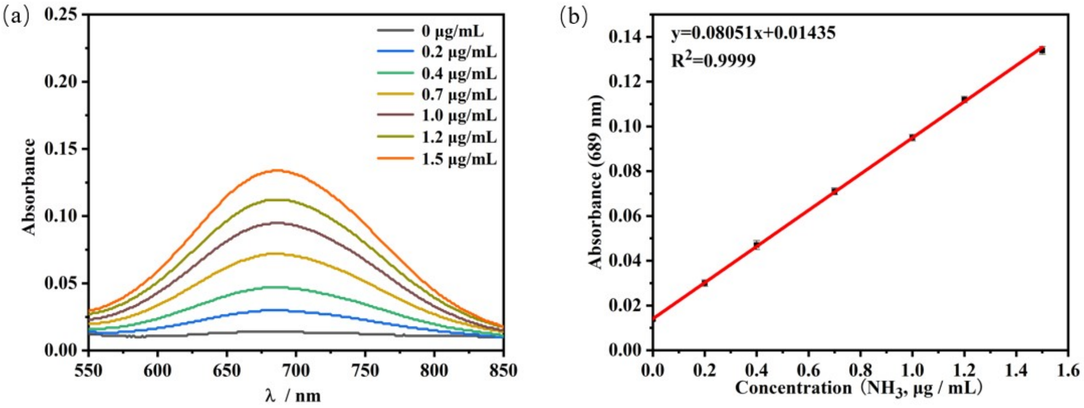

Figure S1. (a) UV-vis absorption spectra of the different concentrations of NH_4Cl solution stained with indophenol indicator after 2 h incubation. (b) Calibration curve of NH_3 plotted by known NH_4^+ concentration.

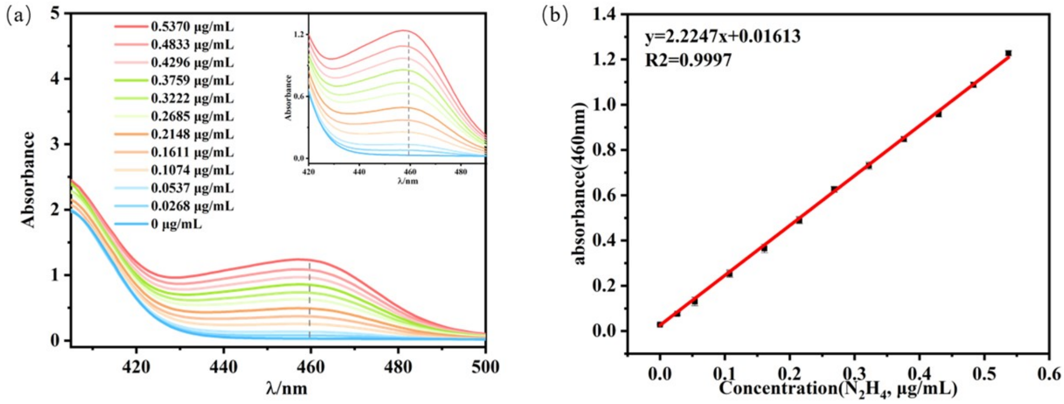

Figure S2. (a) UV-vis absorption spectra of different concentrations of N_2H_4 solution stained with coloring reagent (p-$C_9H_{11}NO$, HCl, and C_2H_5OH) after incubation for 20 min at room temperature. (b) Calibration curve for calculating the N_2H_4 concentration.

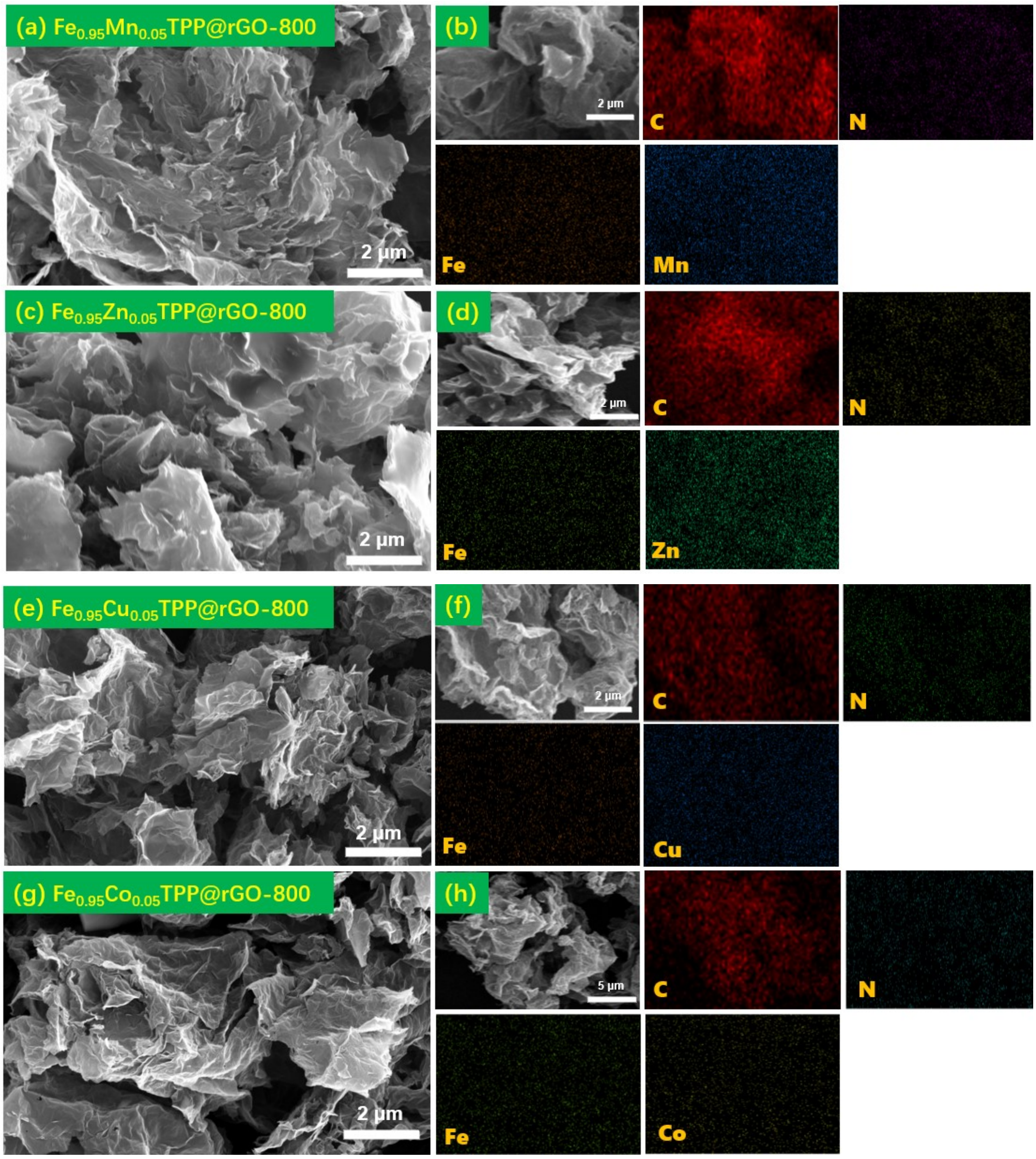

Figure S3. (a,c,e,g) SEM images of $Fe_{0.95}M_{0.05}$TPP@rGO-800 (M=Mn, Zn, Cu, Co) and (b,d,f,h) corresponding EDS mapping images.

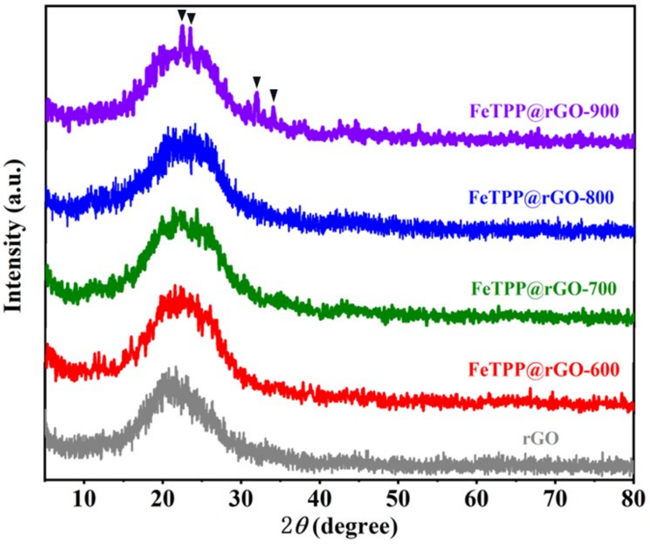

Figure S4. (a) XRD patterns of rGO and FeTPP@rGO-t (t=600/700/800/900).

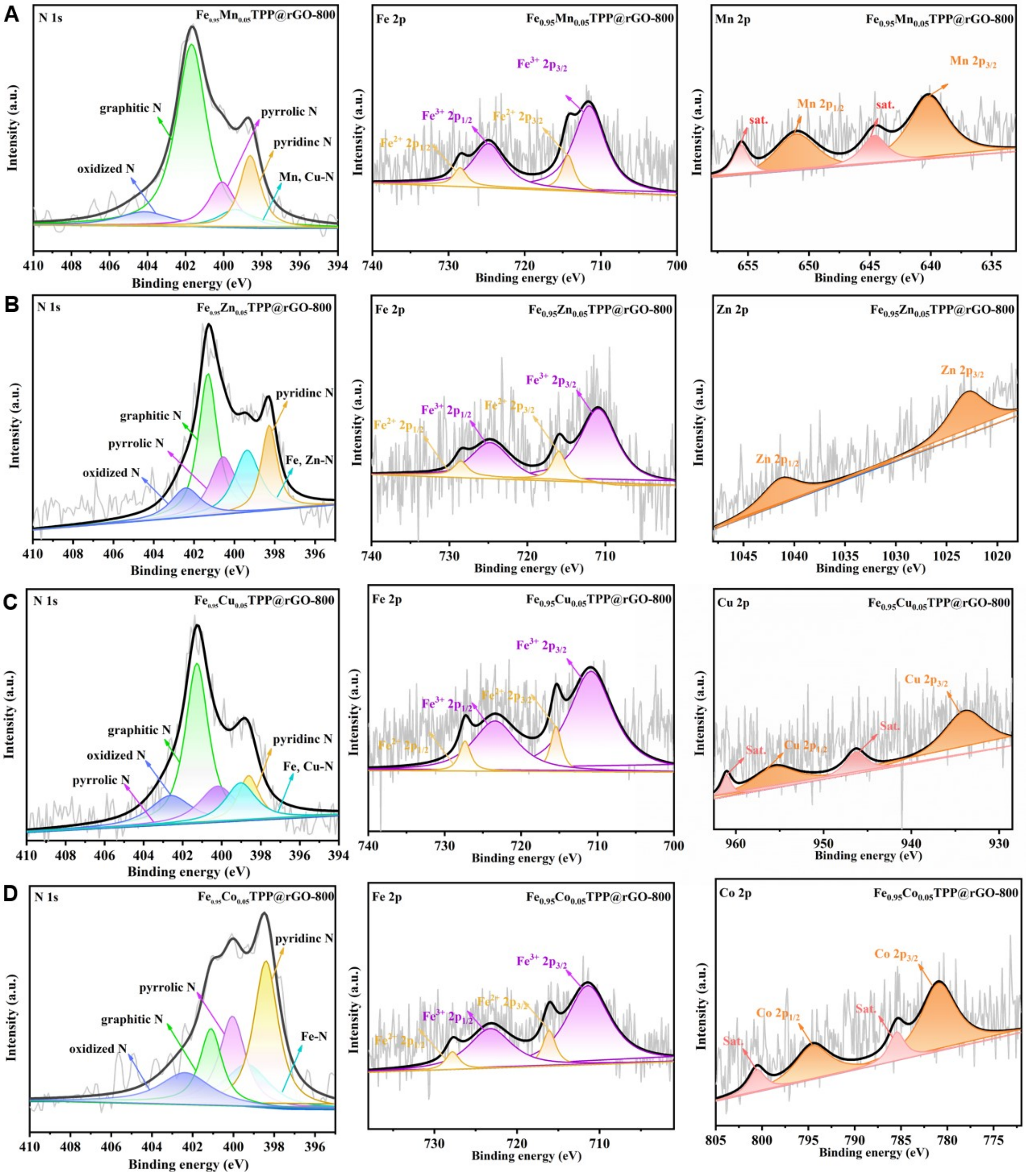

Figure S5. XPS survey spectrum of (A) $Fe_{0.95}Mn_{0.05}$TPP@rGO-800, (A) $Fe_{0.95}Zn_{0.05}$TPP@rGO-800, (A) $Fe_{0.95}Cu_{0.05}$TPP@rGO-800, (A) $Fe_{0.95}Co_{0.05}$TPP@rGO-800.

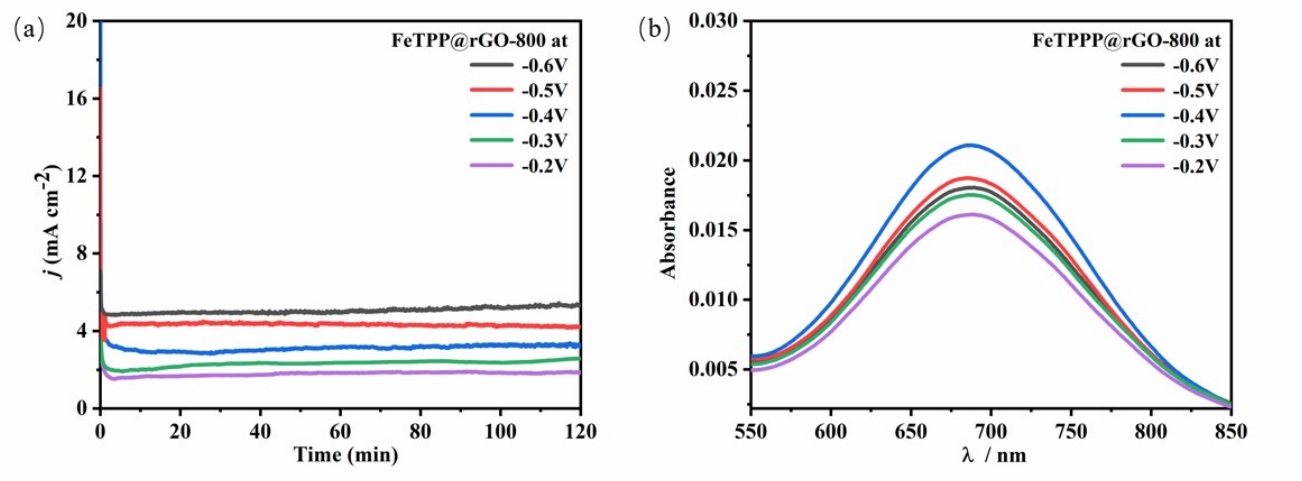

Figure S6. (a) Chronoamperometry curves of FeTPP@rGO-800 recorded in N_2-saturated electrolyte at the given potentials. (b) Corresponding UV-vis absorption spectra of the electrolytes stained with indophenol indicator.

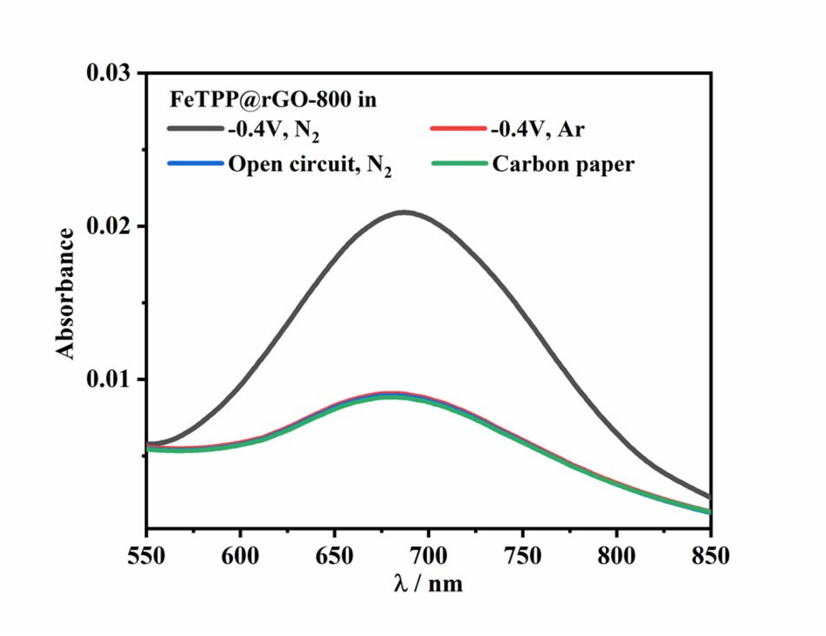

Figure S7. UV-vis absorption spectra of the electrolytes stained with indophenol indicator after 2h potentiostatic electrolysis on FeTPP@rGO-800 in the following conditions: (1) N_2-saturated electrolyte at-0.4 V (all potentials are versus RHE); (2) Ar-saturated electrolyte at-0.4 V; (3) N_2-saturated electrolyte at the open circuit potential; (4) pure carbon paper.

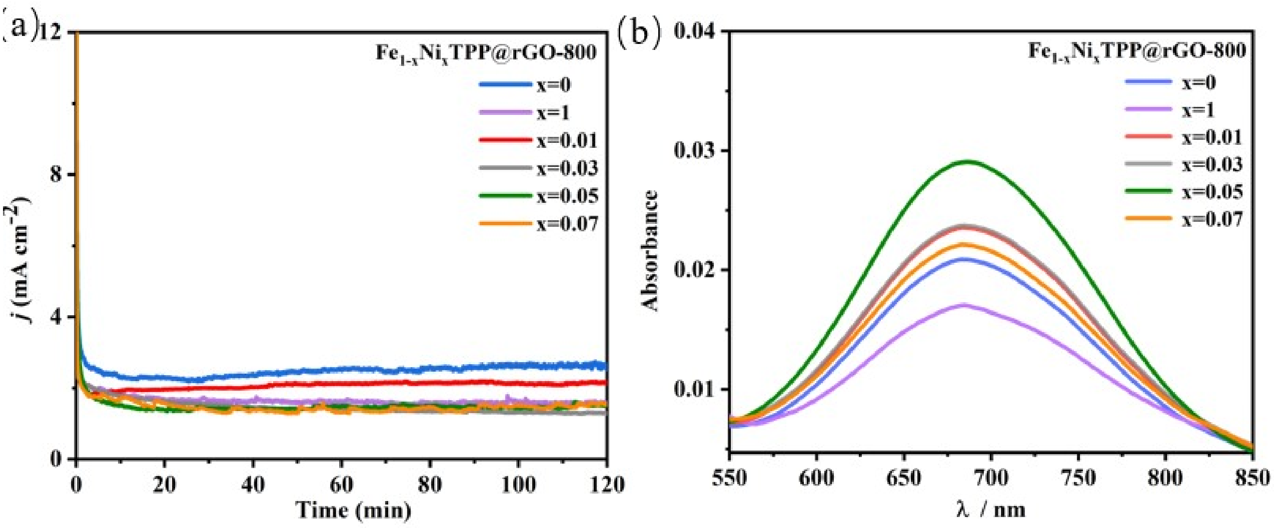

Figure S8. (a) Chronoamperometry curves of $Fe_{1-x}M_xTPP$@rGO-800 recorded in N_2-saturated electrolyte at the potential of -0.4V. (b) Corresponding UV-vis absorption spectra of the electrolytes stained with indophenol indicator.

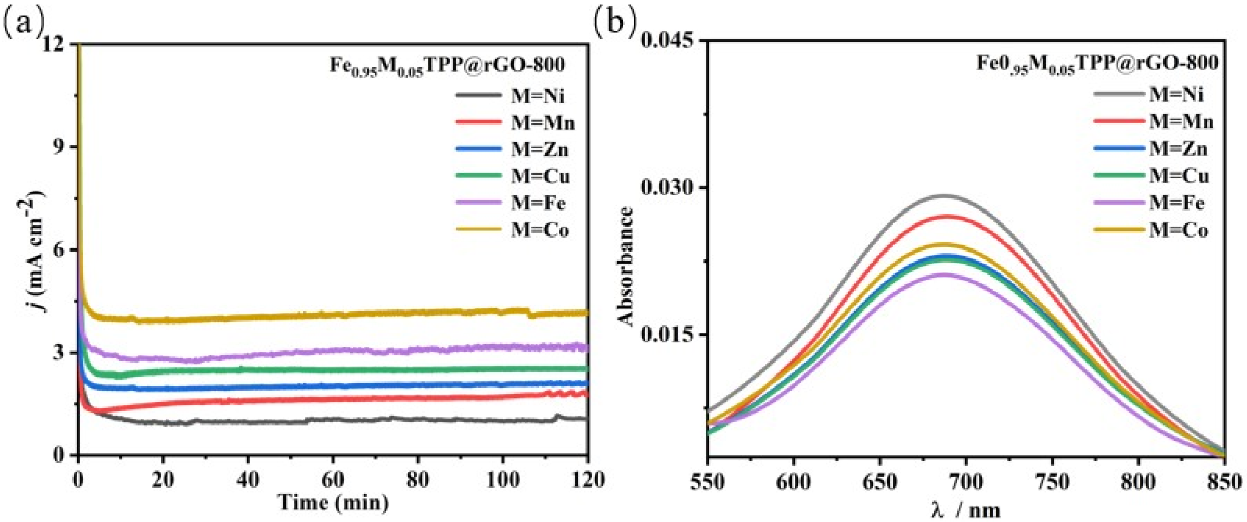

Figure S9. (a) Chronoamperometry curves of $Fe_{0.95}M_{0.05}TPP$@rGO-800 recorded in N_2-saturated electrolyte at the potential of -0.4V. (b) Corresponding UV-vis absorption spectra of the electrolytes stained with indophenol indicator.

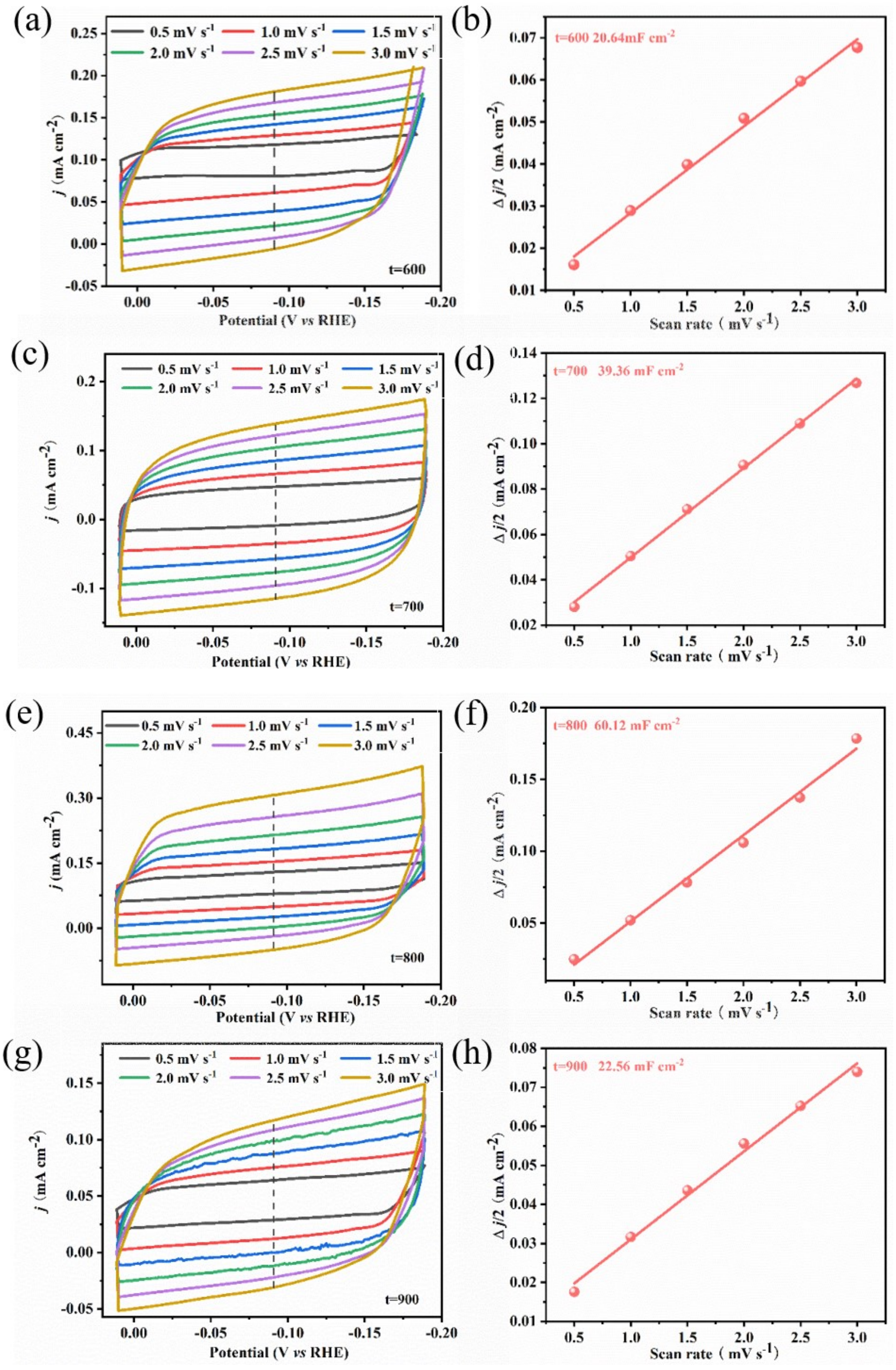

Figure S10. Electrochemical surface area measurement of the FeTPP@rGO-t(t=600/700/800/900) samples using double-layer capacitance. (a, c, e, g) Cyclic voltammograms of FeTPP@rGO-600, FeTPP@rGO-700, FeTPP@rGO-800, FeTPP@rGO-900 at various scan rates from 0.5 to 3 mV s^{-1} in the potential range between 0.01~-0.19 V *vs* RHE. (b, d, f, h) Corresponding double-layer charging current against the scan rate, and the slope of the linear fit is double-layer capacitance.

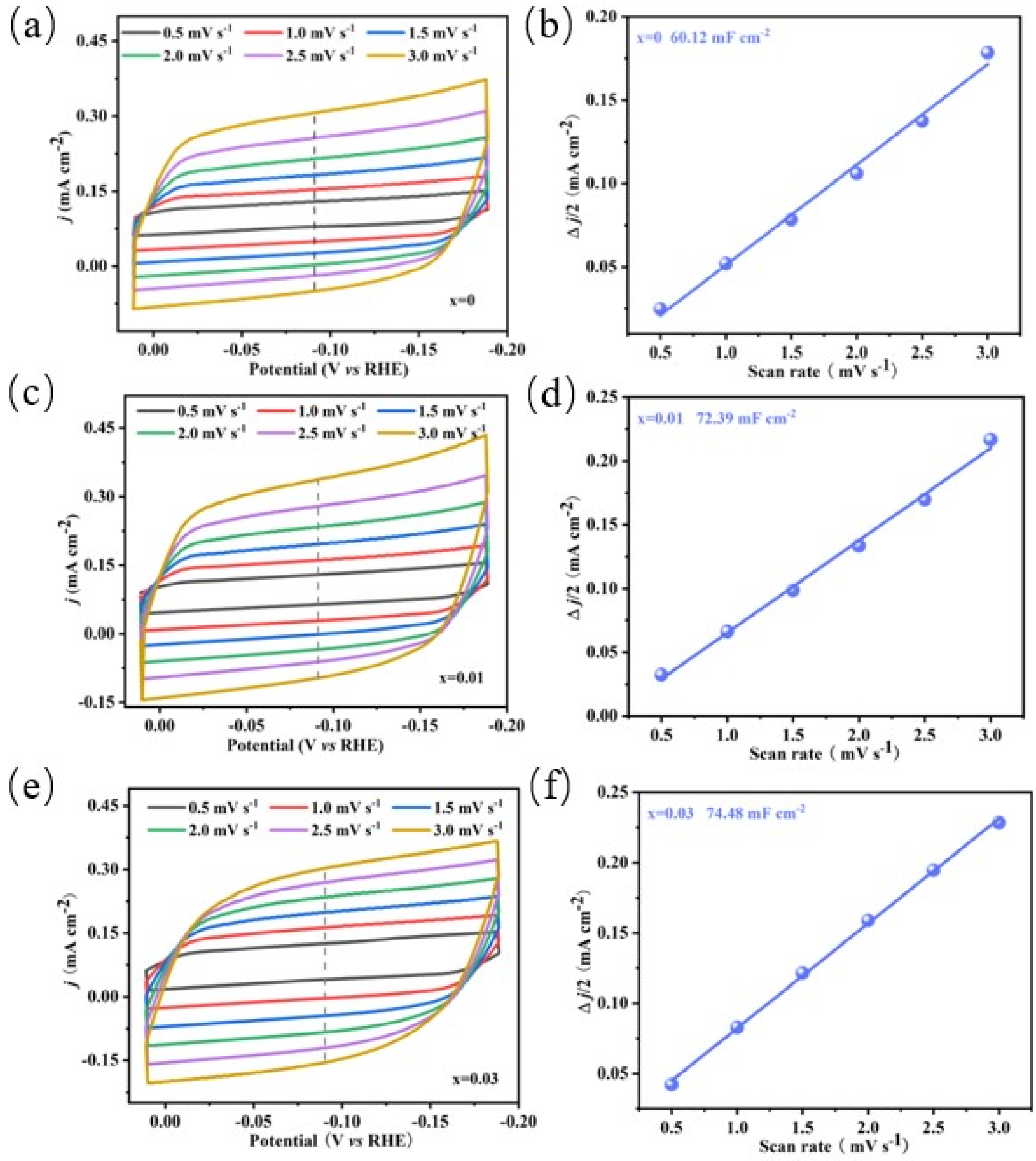
(a)
0.5 mV s-1
1.0 mV s-1
1.5 mV s-1
2.0 mV s-1
2.5 mV s-1
3.0 mV s-1
j (mA cm-2)
0.45
0.30
0.15
0.00
x=0
0.00
-0.05
-0.10
-0.15
-0.20
Potential (V vs RHE)
(b)
x=0 60.12 mF cm-2
Δ j/2 (mA cm-2)
0.20
0.15
0.10
0.05
0.5
1.0
1.5
2.0
2.5
3.0
Scan rate (mV s-1)
(c)
0.5 mV s-1
1.0 mV s-1
1.5 mV s-1
2.0 mV s-1
2.5 mV s-1
3.0 mV s-1
j (mA cm-2)
0.45
0.30
0.15
0.00
-0.15
x=0.01
0.00
-0.05
-0.10
-0.15
-0.20
Potential (V vs RHE)
(d)
x=0.01 72.39 mF cm-2
Δ j/2 (mA cm-2)
0.25
0.20
0.15
0.10
0.05
0.00
0.5
1.0
1.5
2.0
2.5
3.0
Scan rate (mV s-1)
(e)
0.5 mV s-1
1.0 mV s-1
1.5 mV s-1
2.0 mV s-1
2.5 mV s-1
3.0 mV s-1
j (mA cm-2)
0.45
0.30
0.15
0.00
-0.15
x=0.03
0.00
-0.05
-0.10
-0.15
-0.20
Potential (V vs RHE)
(f)
x=0.03 74.48 mF cm-2
Δ j/2 (mA cm-2)
0.25
0.20
0.15
0.10
0.05
0.5
1.0
1.5
2.0
2.5
3.0
Scan rate (mV s-1)

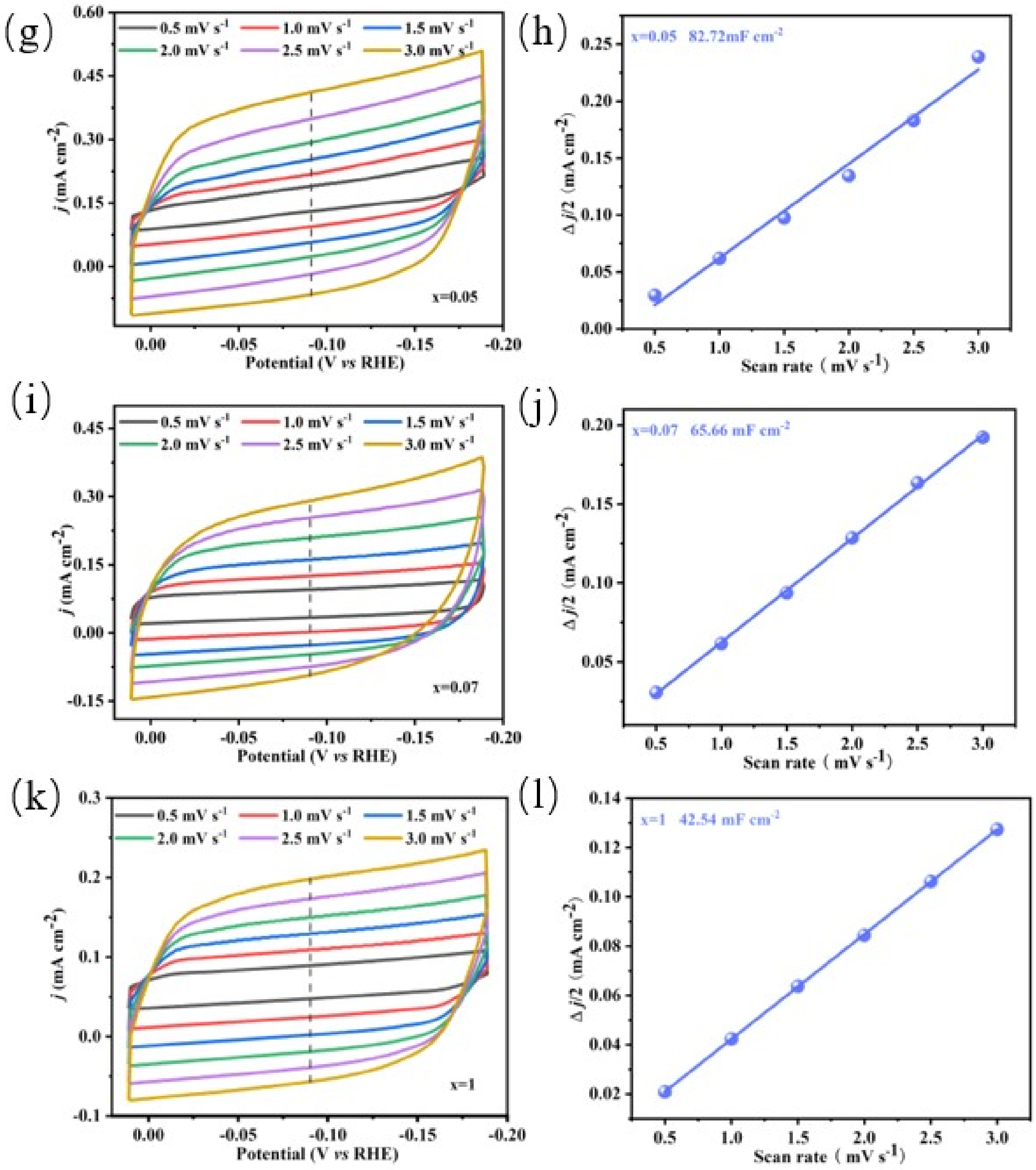

Figure S11. Electrochemical surface area measurement of the $Fe_{1-x}Ni_x$TPP@rGO-800 samples using double-layer capacitance. (a, c, e, g, i, k) Cyclic voltammograms of FeTPP@rGO-800, $Fe_{0.99}Ni_{0.01}$TPP@rGO-800, $Fe_{0.97}Ni_{0.03}$TPP@rGO-800, $Fe_{0.95}Ni_{0.05}$TPP@rGO-800, $Fe_{0.93}Ni_{0.07}$TPP@rGO-800, NiTPP@rGO-800 at various scan rates from 0.5 to 3 mV s^{-1} in the potential range between 0.01~-0.19 V *vs* RHE. (b, d, f, h, j, l) Corresponding double-layer charging current against the scan rate, and the slope of the linear fit is double-layer capacitance.

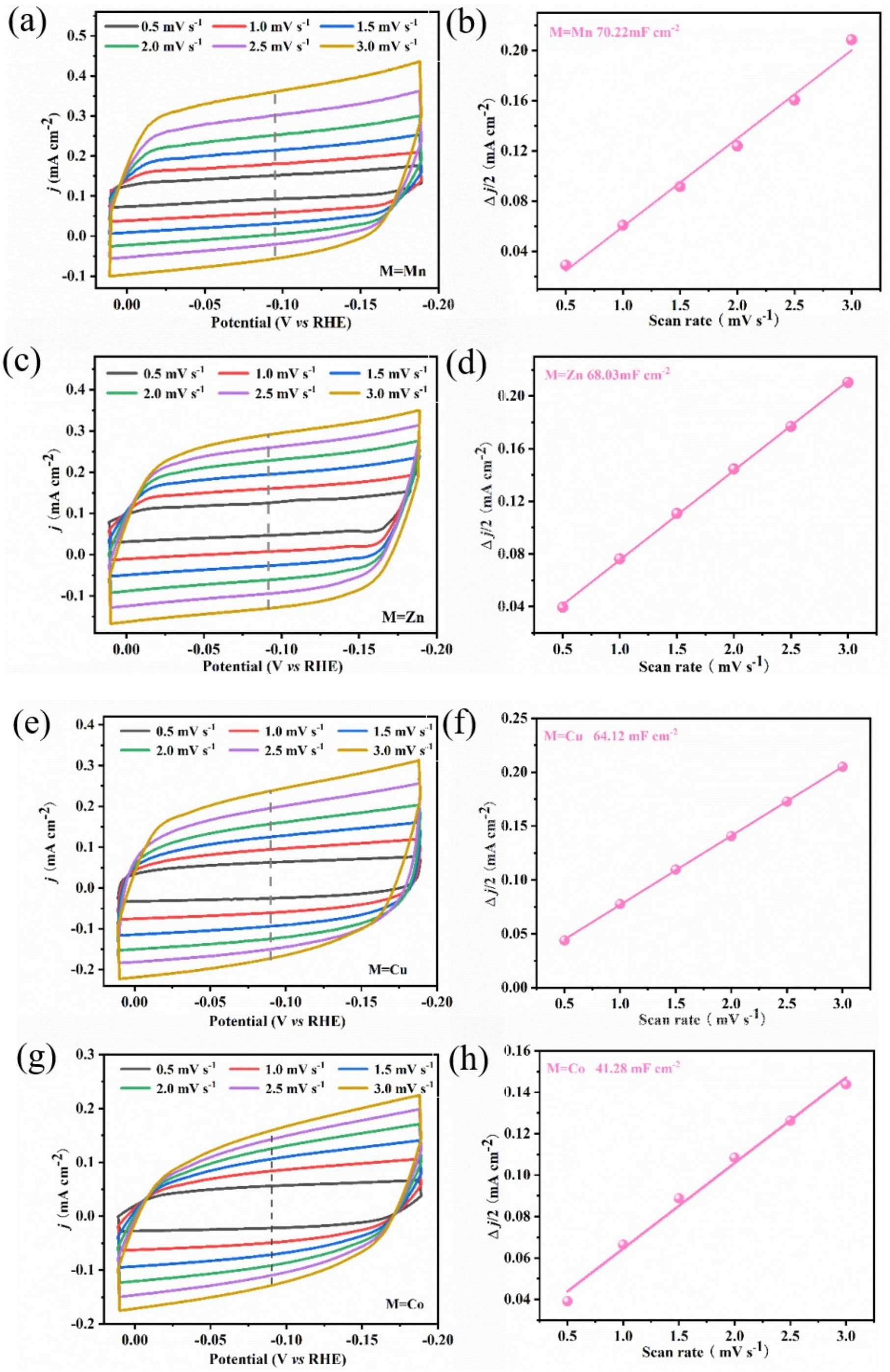

Figure S12. Electrochemical surface area measurement of the $Fe_{0.95}M_{0.05}$TPP@rGO-800(M=Mn, Zn, Cu, Co) samples using double-layer capacitance. (a, c, e, g) Cyclic voltammograms of $Fe_{0.95}Mn_{0.05}$TPP@rGO-800, $Fe_{0.95}Zn_{0.05}$TPP@rGO-800, $Fe_{0.95}Cu_{0.05}$TPP@rGO-800 and $Fe_{0.95}Co_{0.05}$TPP@rGO-800 at various scan rates from 0.5 to 3 mV s^{-1} in the potential range between 0.01~-0.19 V *vs* RHE. (b, d, f, h) Corresponding double-layer charging current against the scan rate, and the slope of the linear fit is double-layer capacitance.

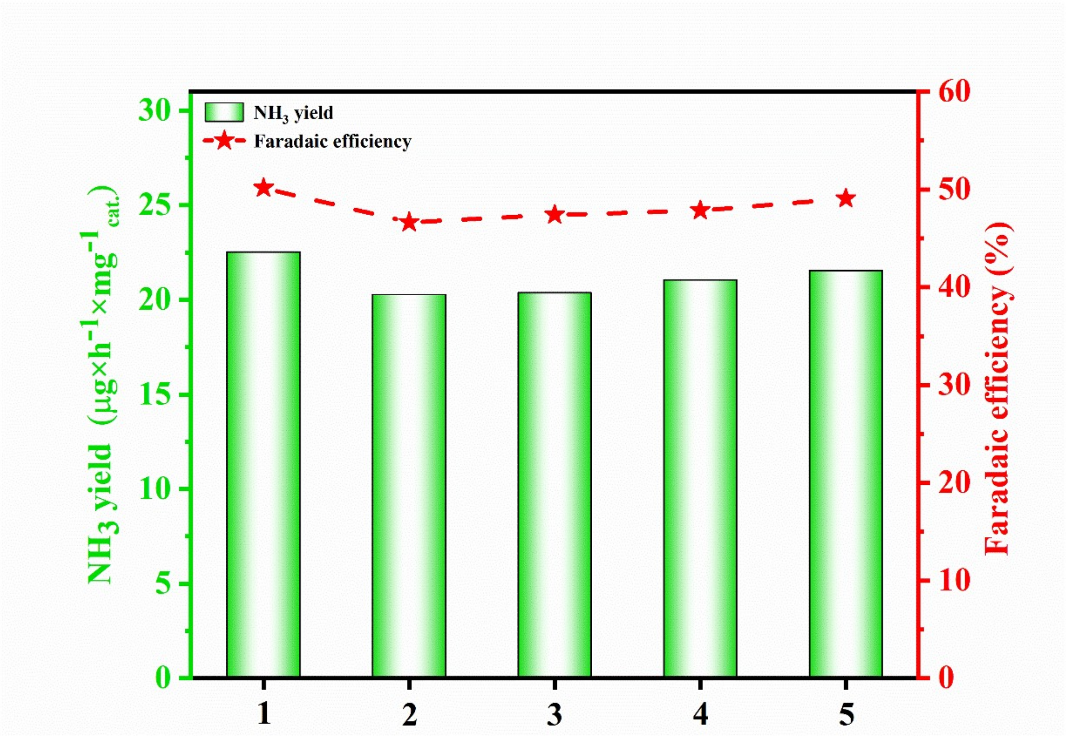

Figure S13. Cycling experiments for $Fe_{0.95}Ni_{0.05}$TPP@rGO-800.

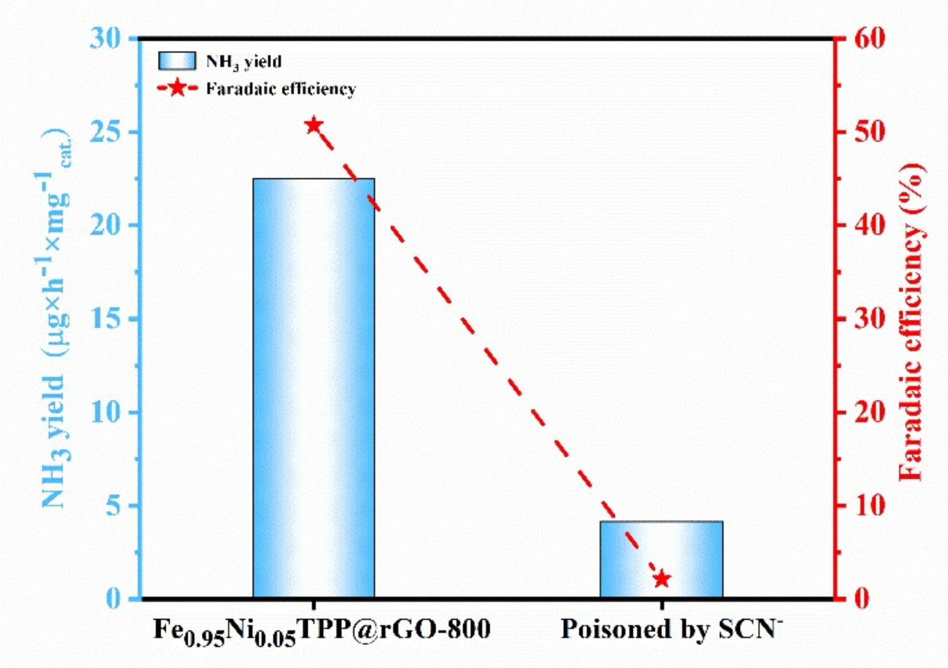

Figure S14. NH_3 yield rate and Faradaic efficiency of $Fe_{0.95}Ni_{0.05}$TPP@rGO-800 before and after SCN^- poisoning.

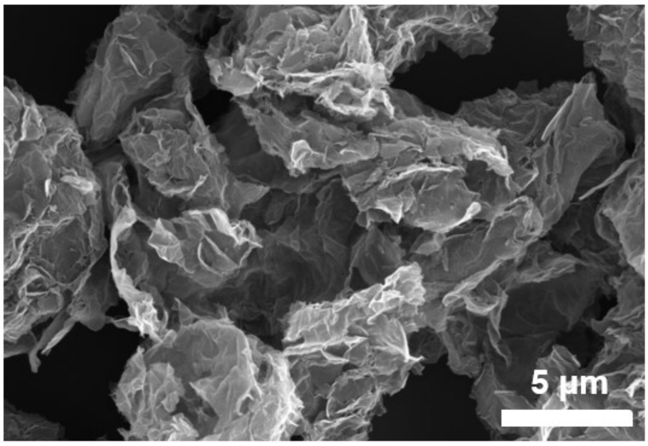

Figure S15. SEM for $Fe_{0.95}Ni_{0.05}$TPP@rGO-800 after 10 h electrolysis test.

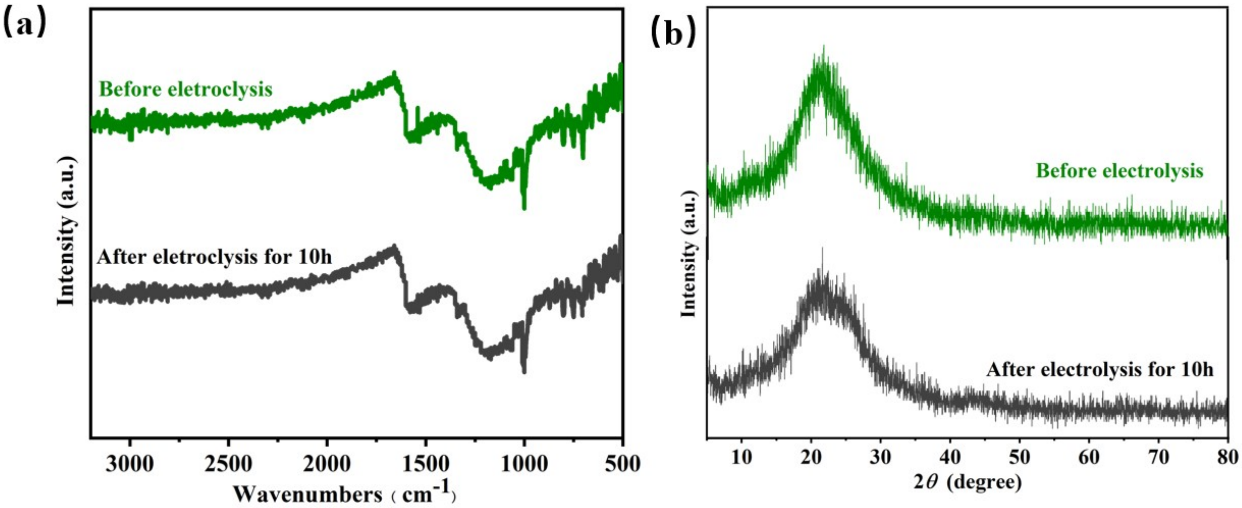

Figure S16. (a) FTIR, (b) XRD of $Fe_{0.95}Ni_{0.05}$TPP@rGO-800 before and after electrolysis for 10 h.